ChemComm

Check for updates

Biosynthesis of multifunctional transformable peptides for downregulation of PD-L1†

Yufei Di,[ab] Zhiwen Yang, [iD][ab] Gang Song, [iD][ab] Qi Shen, [iD][a] Haotian Bai, [iD][a] Yiming Huang, [iD][a] Fengting Lv [iD] *[a] and Shu Wang [iD] *[ab]

Here, we present a biosynthesized material M1 for immune checkpoint blocking therapy. M1 could realize a morphological transformation from globular to fibrous *in situ* in the presence of cathepsin B (CtsB) after entering tumor cells. The GO203 peptides of M1 are exposed, which could bind to mucin 1 (MUC1) to suppress the homodimerization process of MUC1, thereby downregulating PD-L1 expression.

In recent years, significant advancements have been made in the field of cancer immunotherapy, which has made it a prominent treatment modality alongside surgery, chemotherapy, and radiotherapy.[1,2] In contrast to traditional cancer treatments, immunotherapy does not directly target tumor cells, but instead activates the body's immune system to recognize and fight tumor cells.[3,4] Chimeric antigen receptor T-cell immunotherapy (CAR-T)[5–7] and immune checkpoint blocking (ICB)[8–11] have achieved outstanding clinical efficacy, providing a new treatment modality for many types of cancer by reactivating T cells to exert their anti-tumor efficacy. The most common ICB therapies block the programmed cell death 1 (PD1)/PD1 ligand 1 (PD-L1) pathway[12–16] using antibodies, peptides, small molecule drugs, and DNA.[17,18] Nevertheless, the clinical response of the ICB inhibitors is only 10–30%,[19] accompanying severe side effects, owing to non-targeting and unresponsiveness of the inhibitors. Therefore, it is of great significance to explore and develop cancer immunotherapy with high efficiency and low side effects.[20,21]

Researchers are dedicated to the study of downregulating the expression of PD-L1 in cancer cells, strengthening the effect of antitumor immunity.[22] Peptides, small interfering RNAs (siRNA), and small molecule inhibitors can down-regulate PD-L1 expression levels to block the activation of the PD1/PD-L1 pathway,[23–25] which

could reactivate T cells to exert their anti-tumor efficacy, inhibiting tumor proliferation. For instance, GO203 peptide could target mucin 1 (MUC1) in multiple tumor models, suppressing PD-L1 expression levels.[26,27] However, the current strategy was only able to maintain a single sequence, which was non-responsive and could not work specifically in the tumor area.[28,29] Very recently, we reported a biosynthetic peptide-based material (P1) that induced tumor cell apoptosis *in vivo* by decaging the functional peptide moieties with the morphology transformation of this material.[30] Here, we introduced a functional peptide (GO203) to construct peptide-based material M1 by replacing the BAK moiety of P1, inspired by the morphology transformation of nanoparticles *in situ*.[31–34] This enzyme catalytic transformable recombinant protein M1 (H6-T22-GFP-GO203-KLVFF-RGD) integrates multiple functions, consisting of a targeting motif (T22 and RGD),[35,36] imaging segment (GFP), tailoring motif (GFLG), functional region (GO203), β-sheet peptide KLVFF and delivery segment (RGD). M1 possesses the ability of morphological transformation from globular to fibrous *in situ* for downregulating the expression of PD-L1 (Fig. 1). Meanwhile, the control peptide M2 without enzyme-cleavable site GFLG was biosynthesized with the identical method. Peptide M3, the enzyme digestion product of M1, was prepared by standard solid-phase peptide synthesis. Due to the amphiphilic characteristics, M1 was able to self-assemble into nanoparticles. The presence of the CtsB enzyme cleavage site and intermolecular hydrogen bonding allow the nanoparticle structure to transform into nanofibers within the cell, thus releasing GO203 peptide which could bind to MUC1 with an active CQC site to inhibit the homodimerization process of MUC1.[37,38] M1 could down-regulate PD-L1 expression in tumor cells thereby activating anti-tumor immunity. Compared to other strategies, the biosynthesized peptide-based material has not only good biocompatibility, but also tumor-targeted morphology transformation capability to down-regulate PD-L1 expression.

The recombinant protein His-T22-GFP-GO203-KLVFF-RGD was successfully produced in *Escherichia coli Trans B* (DE3),

[a] Beijing National Laboratory for Molecular Sciences, Key Laboratory of Organic Solids, Institute of Chemistry, Chinese Academy of Sciences, Beijing 100190, China. E-mail: wangshu@iccas.ac.cn, lvft@iccas.ac.cn

[b] College of Chemistry, University of Chinese Academy of Sciences, Beijing 100049, China
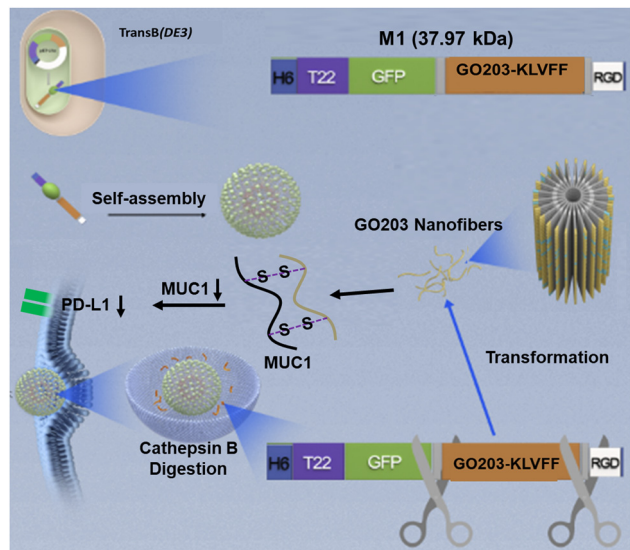
Fig. 1 Schematic illustration of the modular design, expression, and self-assembly behavior of the recombinant protein M1. Morphology transformation of M1 by CtsB enzyme catalysis to form nanofibrous structures for downregulating the intracellular PD-L1 level.

Fig. 2 (a) Hydrodynamic diameter of M1 treated with and without CtsB. (b) CD spectra of M1, and M1 treated with CtsB, as well as M3. (c) Representative TEM images of M1 and M1 in the presence of CtsB (1.0 μg mL^{-1}, acetate buffer, 0.01 M, pH 5.0) for 10 h, respectively. Scale bars, 200 nm.

purified by Ni-NTA affinity chromatography to purify the 6× His-tagged protein products and detected as a single protein species with the expected molecular mass of 37.97 kDa (Fig. S2a, ESI†). The purified peptide M1 exhibited the characteristic fluorescence of GFP with an emission maximum at 520 nm, as depicted in Fig. S1 (ESI†). The successful expression of M1 by bacteria was verified. Meanwhile, the SDS-PAGE assessment of the control peptide M2 was performed and shown in Fig. S2b (ESI†). The molecular transformation of M1 incubated with CtsB was investigated with high-performance liquid chromatography mass spectrometry (LC-MS). A new peak corresponding to M3 in LC-MS as illustrated in Fig. S3 (ESI†) verified that M1 was cleaved by CtsB at the designed digestion site GFLG. Then the enzyme catalytic transformation behavior of the M1 assemblies was examined by transmission electron microscopy (TEM) and circular dichroism (CD). TEM of the purified extracts revealed that the spherical form of M1 was about 60 nm in diameter (Fig. 2c), which was in accordance with the dynamic light scattering (DLS) result of 61.3 ± 9.2 nm (Fig. 2a). There was no spherical to fibrous morphology change of M1 observed after treatment with CtsB for 5 h (Fig. S4, ESI†), while obvious nanofibers were observed with the incubation time up to 10 h, which proved that the morphology of M1 could transform from nanoparticles to nanofibers. On the contrary, the control peptide-based material M2 without CtsB cleavable sites kept the spherical morphology even after the treatment of CtsB for 10 h, which is shown in Fig. S5 (ESI†). The morphology change of M1 was further confirmed by dynamic light scattering measurement, as presented in Fig. 2a, and an obvious positive shift of the particle size of M1 was observed upon the addition of CtsB for 10 h. To investigate the chemical driving force of nanofiber formation, the secondary structure was explored by circular dichroism. After incubation with CtsB for 10 h, the M1 assemblies showed a positive CD signal at 195 nm and negative
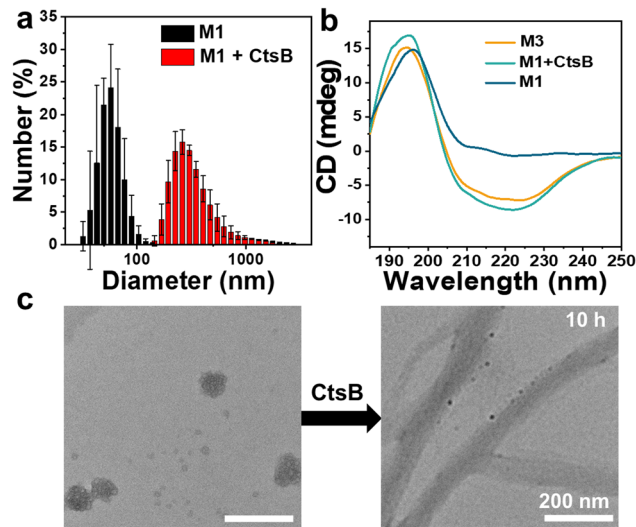
signals at 220 nm, which confirm the typical β-sheet fibrous structure.[39] In contrast, M1 showed a positive band around 195 nm in the absence of CtsB and exhibited a predominant random structure (Fig. 2b). Furthermore, to demonstrate that GO230 could form a complex with MUC1 in cells, MUC1 and GO230 were customized and cocultured. The sulfur crosslinking product of them could be tested by HRMS (Fig. S6, ESI†), proving the successful formation of the GO203-MUC1 fragment complex, which effectively prevents the dimerization of MUC1.

Before investigating the morphological transformation of M1 in living cells, internalization behaviour and biosafety of this peptide were firstly evaluated. For A375 cells treated with 1 mg mL^{-1} M1, their fluorescence enhanced with increasing the incubation time and reached a plateau at 12 h, then maintained the intensity until 24 h, as shown in Fig. S7 (ESI†). It was suggested that efficient cellular uptake of M1 by the cells occurred, which may be ascribed to its superior hydrophilicity. To evaluate the biosafety of M1, A375 cells were incubated with different concentrations of M1. As illustrated in Fig. 3b, the cells showed high survival rates at concentrations up to 1 mg mL^{-1}, which verified its superior biocompatibility. Given that CtsB is mainly distributed in lysosomes,[40] efficient CtsB-catalytic transformation requires lysosomal cellular endocytosis.

To probe the location of M1 in cells, fluorescent co-localization of M1 and lysotracker was performed. As expected, M1 with intensive green fluorescence from GFP shared obvious overlapped fluorescence with lysotracker, which was labelled with red fluorescence (Fig. 3a). These results demonstrated the efficient cellular endocytosis ability and lysosomal location of M1, which satisfy the requirement for CtsB-catalyzed transformation.

Bio-TEM was employed to study the intracellular morphology transformation of M1. After M1 entered the A375 cells, fibrous structures were observed by TEM, as presented in
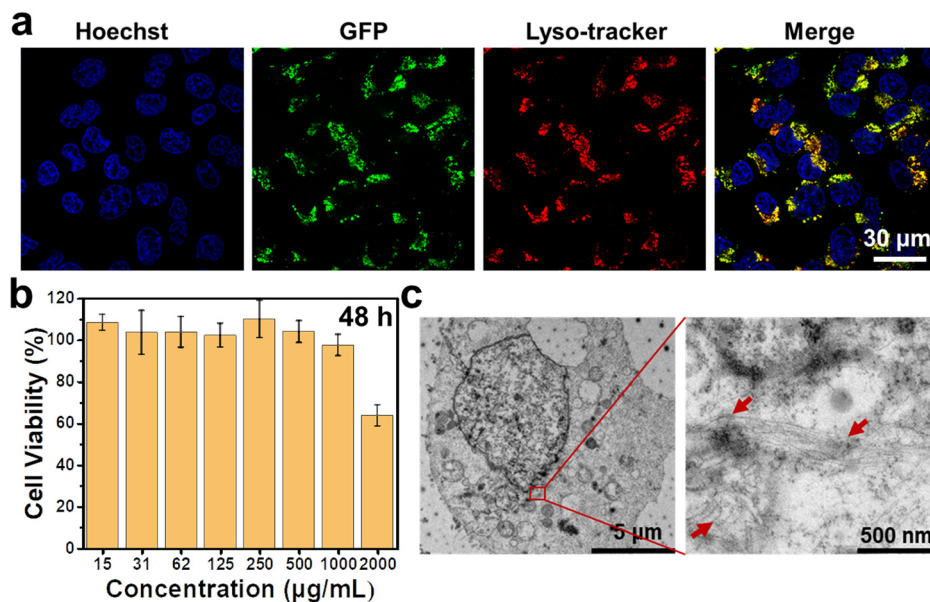
Fig. 3 (a) CLSM images of A375 cells treated with M1 for 24 h. (b) Cell viability of A375 cells incubated with various concentrations of M1 for 48 h. (c) Bio-TEM images of the ultrathin cell sections of M1. The red arrows indicated the nanofibers.

Fig. 3c, while there was no similar structure found for M2-treated cells or PBS-treated cells (Fig. S8, ESI†). The introduction of the enzyme cleavable peptide GFLG was critical for intracellular transformation of M1 to fibrous structures, which was consistent with the phenomenon in solution. As shown in Fig. 4a, both M1 and M2 could reduce the PD-L1 expression level of A375 cells, and M1 displayed a greater degree than M2, indicating that more GO203 moieties were exposed in the presence of CtsB enzyme to bind MUC1, therefore, leading to better suppression of the PD-L1 expression levels (Fig. S9, ESI†). The cellular immunity could recognize and lyse tumor cells, and the PD-1/PD-L1 interaction has been reported to affect T cell functions.[41] We tested our designed peptide M1 for cellular immunity with Jurkat T cells. A375 cells were pretreated with PBS, the single-sequence GO203, M2 and M1 to influence the expression of PD-L1, and subsequently, these A375 cells were cocultured with Jurkat T cells. As illustrated in Fig. 4b, Jurkat T cells killed A375 cells treated with M1 more effectively than those treated with M2 or PBS, which suggested that the designed peptide M1 could downregulate the expression of PD-L1, inducing effective cellular immunity. Moreover, the immunotherapeutic effect of self-assembled GO203 is better than that of single-sequence.

In summary, we have established a biosynthesized protein-based material (M1) with intracellular morphology transformation ability that can effectively downregulate the PD-L1 expression of cancer cells. These findings identify that self-assembly peptide-based materials with morphology transformation ability contribute better immunotherapeutic performance than single sequence and nanostructured GO203, which reduces to some extent the off-target and side effects confronted for clinical immunotherapy. It is believed that better therapeutic performance and more advanced specific biochemical
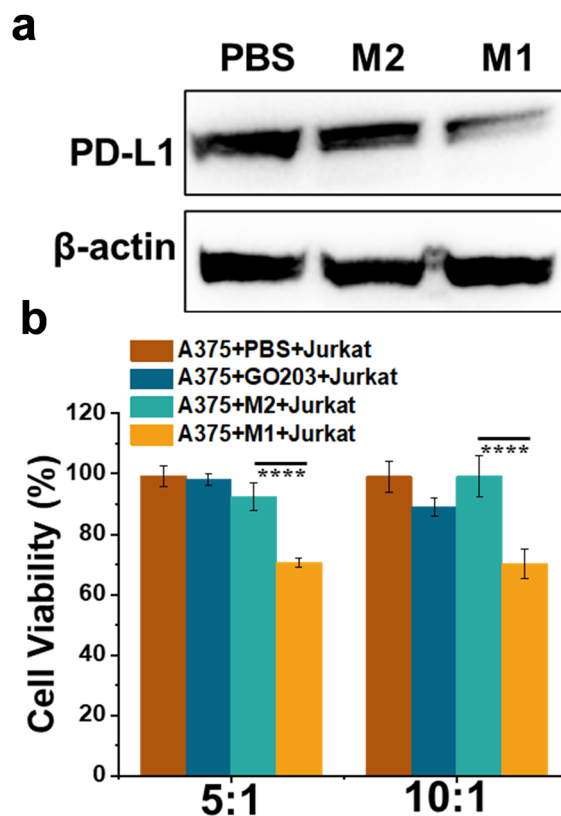

Fig. 4 (a) Western blotting analyses of the expression of PD-L1 in A375 cells under different treatments. (b) Cell viability of A375 cells with Jurkat T cells. Note that the A375 cells were pretreated with PBS, the single-sequence GO203, M2 and M1, respectively.

applications will be presented with further functionalization and integration with other therapeutic modalities.

Data availability

The data supporting this article have been included as part of the ESI.†

Conflicts of interest

There are no conflicts to declare.

Notes and references

1 J. Prieto, I. Melero and B. Sangro, *Nat. Rev. Gastroenterol. Hepatol.*, 2015, **12**, 681–700.
2 A. Nazha and M. A. Sekeres, *Annu. Rev. Med.*, 2017, **68**, 127–137.
3 Daniel S. Chen and I. Mellman, *Immunity*, 2013, **39**, 1–10.
4 B. Bao, Q. Yuan, Q. Feng, L. Li, M. Q. Li and Y. Tang, *CCS Chem.*, 2024, **6**, 693–708.
5 R. C. Larson and M. V. Maus, *Nat. Rev. Cancer*, 2021, **21**, 145–161.
6 A. Rodriguez-Garcia, R. C. Lynn, M. Poussin, M. A. Eiva, L. C. Shaw, R. S. O'Connor, N. G. Minutolo, V. Casado-Medrano, G. Lopez, T. Matsuyama and D. J. Powell, *Nat. Commun.*, 2021, **12**, 877.
7 L. C. Wang, A. Lo, J. Scholler, J. Sun, R. S. Majumdar, V. Kapoor, M. Antzis, C. E. Cotner, L. A. Johnson, A. C. Durham, C. C. Solomides, C. H. June, E. Puré and S. M. Albelda, *Cancer Immunol. Res.*, 2014, **2**, 154–166.
8 P. Sharma and J. P. Allison, *Science*, 2015, **348**, 56–61.
9 Y. Yang, J. Xu, Y. Sun, L. Mo, B. Liu, X. Pan, Z. Liu and W. Tan, *J. Am. Chem. Soc.*, 2021, **143**, 8391–8401.
10 C. Wang, J. Wang, X. Zhang, S. Yu, D. Wen, Q. Hu, Y. Ye, H. Bomba, X. Hu, Z. Liu, G. Dotti and Z. Gu, *Sci. Transl. Med.*, 2018, **10**, eaan3682.
11 L. Barrueto, F. Caminero, L. Cash, C. Makris, P. Lamichhane and R. R. Deshmukh, *Transl. Oncol.*, 2020, **13**, 100738.
12 A. Mantovani, F. Marchesi, A. Malesci, L. Laghi and P. Allavena, *Nat. Rev. Clin. Oncol.*, 2017, **14**, 399–416.
13 S. Rafiq, O. O. Yeku, H. J. Jackson, T. J. Purdon, D. G. van Leeuwen, D. J. Drakes, M. Song, M. M. Miele, Z. Li, P. Wang, S. Yan, J. Xiang, X. Ma, V. E. Seshan, R. C. Hendrickson, C. Liu and R. J. Brentjens, *Nat. Biotechnol.*, 2018, **36**, 847–856.
14 J. Pan, X. Li, B. Shao, F. Xu, X. Huang, X. Guo and S. Zhou, *Adv. Mater.*, 2022, **34**, 2106307.
15 Z. Xiao, Z. Su, S. Han, J. Huang, L. Lin and X. Shuai, *Sci. Adv.*, 2020, **6**, eaay7785.
16 Y. Chao and Z. Liu, *Nat. Rev. Bioeng.*, 2023, **1**, 125–138.
17 A. Ribas and J. D. Wolchok, *Science*, 2018, **359**, 1350–1355.
18 Y. Zhai, J. Wang, T. Lang, Y. Kong, R. Rong, W. Cai, W. Ran, F. Xiong, C. Zheng, Y. Wang, Y. Yu, H. H. Zhu, P. Zhang and Y. Li, *Nat. Nanotechnol.*, 2021, **16**, 1271–1280.
19 J. E. Rosenberg, J. Hoffman-Censits, T. Powles, M. S. van der Heijden, A. V. Balar, A. Necchi, N. Dawson, P. H. O'Donnell, A. Balmanoukian, Y. Loriot, S. Srinivas, M. M. Retz, P. Grivas, R. W. Joseph, M. D. Galsky, M. T. Fleming, D. P. Petrylak, J. L. Perez-Gracia, H. A. Burris, D. Castellano, C. Canil, J. Bellmunt, D. Bajorin, D. Nickles, R. Bourgon, G. M. Frampton, N. Cui, S. Mariathasan, O. Abidoye, G. D. Fine and R. Dreicer, *Lancet*, 2016, **387**, 1909–1920.
20 E. Zhang, Y. Chen, F. Lv, Z. Zuo, F. He, Y. Li, Y. Huang, Y. Li and S. Wang, *CCS Chem.*, 2023, **6**, 641–651.
21 P. Sharma and J. P. Allison, *Cell*, 2015, **161**, 205–214.
22 H. Li, C.-W. Li, X. Li, Q. Ding, L. Guo, S. Liu, C. Liu, C.-C. Lai, J.-M. Hsu, Q. Dong, W. Xia, J. L. Hsu, H. Yamaguchi, Y. Du, Y.-J. Lai, X. Sun, P. B. Koller, Q. Ye and M.-C. Hung, *Gastroenterology*, 2019, **156**, 1849–1861.
23 S. Yang, M. K. Shim, W. J. Kim, J. Choi, G.-H. Nam, J. Kim, J. Kim, Y. Moon, H. Y. Kim, J. Park, Y. Park, I.-S. Kim, J. H. Ryu and K. Kim, *Biomaterials*, 2021, **272**, 120791.
24 X. Guan, L. Sun, Y. Shen, F. Jin, X. Bo, C. Zhu, X. Han, X. Li, Y. Chen, H. Xu and W. Yue, *Nat. Commun.*, 2022, **13**, 2834.
25 M. Mamuti, Y. Wang, Y.-D. Zhao, J.-Q. Wang, J. Wang, Y.-L. Fan, W.-Y. Xiao, D.-Y. Hou, J. Yang, R. Zheng, H.-W. An and H. Wang, *Adv. Mater.*, 2022, **34**, 2109432.
26 T. Maeda, M. Hiraki, C. Jin, H. Rajabi, A. Tagde, M. Alam, A. Bouillez, X. Hu, Y. Suzuki, M. Miyo, T. Hata, K. Hinohara and D. Kufe, *Cancer Res.*, 2018, **78**, 205–215.
27 A. Bouillez, D. Adeegbe, C. Jin, X. Hu, A. Tagde, M. Alam, H. Rajabi, K.-K. Wong and D. Kufe, *OncoImmunology*, 2017, **6**, e1338998.
28 J. Dai, J.-J. Hu, X. Dong, B. Chen, X. Dong, R. Liu, F. Xia and X. Lou, *Angew. Chem., Int. Ed.*, 2022, **61**, e202117798.
29 H. Yao, J. Lan, C. Li, H. Shi, J.-P. Brosseau, H. Wang, H. Lu, C. Fang, Y. Zhang, L. Liang, X. Zhou, C. Wang, Y. Xue, Y. Cui and J. Xu, *Nat. Biomed. Eng.*, 2019, **3**, 306–317.
30 Y. Di, Q. Shen, Z. Yang, T. Fang, Y. Liu, Y. Liu, G. Song, Q. Luo, F. Wang, X. Yan, H. Bai, Y. Huang, F. Lv and S. Wang, *Small*, 2023, **19**, 2303035.
31 H. He, S. Liu, D. Wu and B. Xu, *Angew. Chem., Int. Ed.*, 2020, **59**, 16445–16450.
32 Y. Di, E. Zhang, Z. Yang, Q. Shen, X. Fu, G. Song, C. Zhu, H. Bai, Y. Huang, F. Lv, L. Liu and S. Wang, *Angew. Chem., Int. Ed.*, 2022, **61**, e202116457.
33 X. Liu, W. Zhan, G. Gao, Q. Jiang, X. Zhang, H. Zhang, X. Sun, W. Han, F.-G. Wu and G. Liang, *J. Am. Chem. Soc.*, 2023, **145**, 7918–7930.
34 D.-B. Cheng, D. Wang, Y.-J. Gao, L. Wang, Z.-Y. Qiao and H. Wang, *J. Am. Chem. Soc.*, 2019, **141**, 4406–4411.
35 U. Unzueta, M. V. Cespedes, N. Ferrer-Miralles, I. Casanova, J. Cedano, J. L. Corchero, J. Domingo-Espin, A. Villaverde, R. Mangues and E. Vazquez, *Int. J. Nanomed.*, 2012, **7**, 4533–4544.
36 L. Sanchez-Garcia, N. Serna, P. Alamo, R. Sala, V. Cespedes, M. Roldan, A. Sanchez-Chardi, U. Unzueta, I. Casanova, R. Mangues, E. Vazquez and A. Villaverde, *J. Controlled Release*, 2018, **274**, 81–92.
37 D. Raina, M. Kosugi, R. Ahmad, G. Panchamoorthy, H. Rajabi, M. Alam, T. Shimamura, G. I. Shapiro, J. Supko, S. Kharbanda and D. Kufe, *Mol. Cancer Ther.*, 2011, **10**, 806–816.
38 M. Hasegawa, R. K. Sinha, M. Kumar, M. Alam, L. Yin, D. Raina, A. Kharbanda, G. Panchamoorthy, D. Gupta, H. Singh, S. Kharbanda and D. Kufe, *Clin. Cancer Res.*, 2015, **21**, 2338–2347.
39 P.-P. Yang, Q. Luo, G.-B. Qi, Y.-J. Gao, B.-N. Li, J.-P. Zhang, L. Wang and H. Wang, *Adv. Mater.*, 2017, **29**, 1605869.
40 X. Ai, C. J. H. Ho, J. Aw, A. B. E. Attia, J. Mu, Y. Wang, X. Wang, Y. Wang, X. Liu, H. Chen, M. Gao, X. Chen, E. K. L. Yeow, G. Liu, M. Olivo and B. Xing, *Nat. Commun.*, 2016, **7**, 10432.
41 J. Bu, A. Nair, M. Iida, W.-J. Jeong, M. J. Poellmann, K. Mudd, L. J. Kubiatowicz, E. W. Liu, D. L. Wheeler and S. Hong, *Nano Lett.*, 2020, **20**, 4901–4909.